Tungsten−Tungsten Multiple-Bond Functionalities Supported by a Polyoxo Surface Modeled by Calix[4]arene

Luca Giannini, Euro Solari, and Carlo Floriani*

Institut de Chimie Minérale et Analytique, BCH, Université de Lausanne, CH-1015 Lausanne, Switzerland

Nazzareno Re

Facoltà di Farmacia, Università degli Studi "G. D'Annunzio", I-66100 Chieti, Italy

Angiola Chiesi-Villa and Corrado Rizzoli

Dipartimento di Chimica, Università di Parma, I-43100 Parma, Italy

Received October 5, 1998

This report deals with the stepwise reduction of the parent compound [*cis*-Cl_2W{*p*-Bu^t-calix[4]-$(O)_4$}], **2**, leading to metal−metal-bonded metalla-calix[4]arene dimers containing the W═W, W≡W, and W$^{\frac{4}{}}$W functionalities. The reduction of **2** with 1 equiv of K led to a W(V) derivative with an unchanged W-coordination sphere in [*cis*-Cl_2W{*p*-Bu^t-calix[4]-$(O)_4$}K], **4**, where the alkali metal cation, hosted inside the cavity, experiences η^6-interactions with the arene rings. The reduction of **2** with 2 equiv of Na led to the dianion $[W_2(\mu\text{-Cl})_2\{p\text{-Bu}^t\text{-calix[4]-(O)}_4\}_2]^{2-}$, hosting two sodium cations inside the calix[4]arene cavities in $[W_2(\mu\text{-Cl})_2\{p\text{-Bu}^t\text{-calix[4]-(O)}_4\}_2Na_2]$, **5** [W−W 2.614(1) Å]. A neutral W═W-calix[4]arene dimer was generated by photochemical labilization of ethylene from $[(\eta^2\text{-}C_2H_4)W\{p\text{-Bu}^t\text{-calix[4]-(O)}_4\}]$ and isolated as the Bu^{t}NC adduct $[W_2\{\mu\text{-}p\text{-Bu}^t\text{-calix[4]-(O)}_4\}_2(Bu^tNC)_2]$, **7** [W−W 2.582(1) Å], containing a bridging oxygen from each calix[4]arene ligand. Further reduction of **5** or the reduction of **2** with 3 equiv of Na led to $[W_2\{p\text{-Bu}^t\text{-calix[4]-(O)}_4\}_2(\mu\text{-Na})_2]$, **8** [W−W 2.313(1) Å], containing two sodium cations shared by the two calix[4]arene ligands. Further reduction of **8** led to $[W_2\{p\text{-Bu}^t\text{-calix[4]-(O)}_4\}_2(\mu\text{-Na})_4]$, **9** [W−W 2.292(1) Å], containing four bridging sodium cations. All the species reported occur in the ion-pair form with the alkali metal cation complexed either in the cavity or at the lower rim of calix[4]arene ligand. The additional solvent molecules around the alkali metal cation are not specified in this abstract. Extended Hückel calculations have been performed to elucidate the electronic configuration of the metal−metal functionalities when sandwiched by two calix[4]arene tetraanions.

Introduction

The relevance of the metal−metal multiple-bond functionality has been exhaustively covered in the classical book by Cotton and Walton.[1] The chemistry of this functionality is strongly associated with the nature of the donor atoms and the coordination geometry imposed by the ancillary ligands. This is particularly true in group VI metal−metal bond chemistry supported by alkoxo ligands,[2] which has been greatly developed in the past decade, mainly by Chisholm's group. We investigated the effect of using the calix[4]arene tetraanion as supporting ligand on the formation and reactivity of metal−metal bonds. A few previous reports deal with the preparation of M−M-bonded complexes supported by multidentate O-donor ligands.[3] In all of them, however, the synthetic strategy was that of ligand substitution from complexes already possessing the multiple M−M bond, and in the kinetic products at least one ligand was found to bridge the two metal centers with two different O atoms. In the context of a detailed study on ligand substitution chemistry at dimetal centers, Chisholm has shown how chelating isomers can be obtained heating in pyridine-bridged species.[4] Such a behavior was recently reported by the same author also using [*p*-Bu^t-calix[4]-$(OH)_4$] as the multidentate O-donor ligand.[5]

On the other hand, we decided to study the reduction chemistry of the parent compound [*cis*-Cl_2W{*p*-Bu^t-calix[4]-$(O)_4$}], **2**, with the aim of generating reactive fragments, namely neutral d^2-W(IV)− and monoanionic d^3-W(III)−tetraoxo species. We expected them to couple to give metal−metal-bonded species or, competitively, to react with suitable substrates to

* To whom correspondence should be addressed.

(1) Cotton, F. A.; Walton, R. A. *Multiple Bonds Between Metal Atoms*, 2nd ed.; Clarendon: Oxford, U.K., 1993.

(2) Chisholm, M. H. *J. Chem. Soc., Dalton Trans.* **1996**, 1781. Chisholm, M. H. *Acc. Chem. Res.* **1990**, *23*, 419. Chisholm, M. H.; Rothwell, I. P. In *Comprehensive Coordination Chemistry*; Wilkinson, G., Gillard, R. G., McCleverty, J. A., Eds.; Pergamon: Oxford, U.K., 1987; Vol. 2, Chapter 15.3. Chisholm, M. H. *Angew. Chem., Int. Ed. Engl.* **1986**, *25*, 21.

(3) Budzichowski, T. A.; Chacon, S. T.; Chisholm, M. H.; Feher, F. J.; Sreib, W. *J. Am. Chem. Soc.* **1991**, *113*, 689. Chisholm, M. H.; Parkin, I. P.; Folting, K.; Lubkovsky, E. B.; Streib, W. E. *J. Chem. Soc., Chem. Commun.* **1991**, 1673.

(4) Chisholm, M. H.; Parkin, I. P.; Folting, K.; Lobkovsky, E. *Inorg. Chem.* **1997**, *36*, 1636. Chisholm, M. H.; Huang, J.-H.; Huffman, J. C.; Parkin, I. P. *Inorg. Chem.* **1997**, *36*, 1642. Chisholm, M. H.; Folting, K.; Streib, W. E.; Wu, D.-D. *Inorg. Chem.* **1998**, *37*, 50.

(5) Chisholm, M. H.; Folting, K.; Streib, W. E.; Wu, D.-D. *Chem. Commun.* **1998**, 379.

10.1021/ic9811796 CCC: $18.00
Published on Web 03/12/1999

Scheme 1

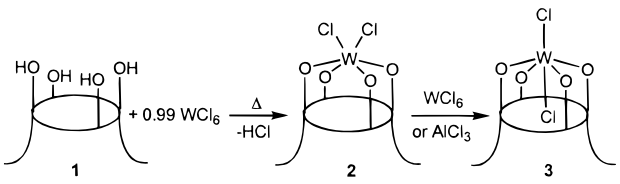

give organometallic derivatives. This report deals in detail with the former ones, which have been briefly communicated.[6]

Experimental Section

All operations were carried out under an atmosphere of purified nitrogen. All solvents were purified by standard methods and freshly distilled prior to use. NMR spectra were recorded on 200-AC and DPX-400 Bruker instruments. Magnetic susceptibility measurements were made with a MPMS5 SQUID susceptometer (Quantum Design Inc.) operating at a magnetic field strength of 1−5 kG. Corrections were applied for diamagnetism calculated from Pascal's constants. Effective magnetic moments were calculated by the equation $\mu_{eff} = 2.828(\chi_M T)^{1/2}$, where χ_M is the magnetic susceptibility per metal atom. Magnetic susceptibility data were collected in the temperature range 2−300 K. **1** (see Scheme 1) was prepared according to the literature procedure.[7] The synthesis of **6** has been described.[8] Sodium and potassium sand[9] were used for the reduction. Bu^{t}NC was purchased from Fluka.

Synthesis of 2. WCl_6 (54.1 g, 136.4 mmol) was added to a suspension of **1** (89.8 g, 138 mmol) in toluene (600 mL) and the resulting suspension refluxed overnight (*Caution!* HCl evolved—risk of foaming during heating before reflux temperature). The solid was collected on an extractor and extracted with Et_2O (450 mL) over 24 h. A bit of black solid was left on the extractor and was discarded. Et_2O was removed in vacuo, toluene (300 mL) was added to the residue, and the resulting suspension was refluxed overnight. After 24 h of standing at room temperature, black microcrystalline **2**·2C_7H_8 was collected and dried in vacuo (133 g, 90%). Anal. Calcd for $C_{58}H_{68}Cl_2O_4W$: C, 64.27; H, 6.32. Found: C, 64.33; H, 6.64. ^{1}H NMR ($CDCl_3$, 298 K, ppm): δ 7.37 (s, 4H, Ar H), 7.3−7.2 (m, 10H, tol), 7.16 (s, 4H, Ar H), 4.84 (d, J = 14.0 Hz, 4H, endo CH_2), 3.57 (d, J = 14.0 Hz, 4H, exo CH_2), 2.4 (s, 6H, tol), 1.43 (s, 18H, Bu^t), 1.25 (s,18H, Bu^t).

Synthesis of 3. $AlCl_3$ (0.124 g, 0.93 mmol) was added to a suspension of **2**·2C_7H_8 (10.12 g, 9.34 mmol) in toluene (200 mL), and the mixture was stirred at room temperature for 4 d. The solid was then collected on an extractor, washed, and extracted with its mother liquor for 5 h. Black **3**·0.5C_7H_8, left on the septum, was then dried in vacuo (7.6 g, 86%). Anal. Calcd for $C_{47.5}H_{56}Cl_2O_4W$: C, 60.3; H, 5.97. Found: C, 60.37; H, 5.93. ^{1}H NMR (C_6D_6, 298 K, ppm): δ 7.15 (s, 8H, Ar H), 4.81 (d, J = 12.8 Hz, 4H, endo CH_2), 3.44 (d, J = 12.8 Hz, 4H, exo CH_2), 2.10 (s, 1.5H, tol), 1.11 (s, 36H, Bu^t).

Synthesis of 4. **2**·2C_7H_8 (22.2 g, 20.48 mmol) was stirred with K (0.8 g, 20.46 mmol) in THF (200 mL) overnight. The resulting red cloudy mixture was filtered, and the filtrate was concentrated in vacuo to half of the volume, whereupon solid started to fall out of solution. Et_2O (250 mL) was then added to the THF suspension and the mixture was stirred overnight, yielding orange crystalline **4**·2.5C_4H_8O·0.5$C_4H_{10}O$, which was collected and dried in vacuo (17.5 g, 74%). Anal. Calcd for $C_{56}H_{77}Cl_2KO_7W$: C, 58.18; H, 6.71. Found: C, 58.2; H, 6.86. ^{1}H NMR (CD_3CN, 298 K, ppm): δ 22 (bd), 12 (s, 4H), 5.35 (s, 4H), 3.56 (m, THF), overlapping with 3.51 (s), 3.32 (q, 2H, Et_2O), 1.71 (m, 10H, THF), 1.26 (s, 18H, Bu^t), 1.18 (s, 18H, Bu^t), 1.03 (t, 3H, Et_2O). Crystals suitable for X-ray analysis were grown from a THF solution at room temperature. μ_{eff} = 1.3−1.9 μ_B in the range 1.9−300 K.

Synthesis of 5. $NaC_{10}H_8$ (45 mL, 0.315 N in THF, 14.2 mmol) was added dropwise to a THF (100 mL) suspension of **2**·2C_7H_8 (7.60 g, 7.01 mmol) at −60 °C. The resulting green mixture turned brown warming up to −30 °C over 3 h. $NaC_{10}H_8$ (6.5 mL, 0.315 N in THF, 2.05 mmol) was added, and the mixture became green. The mixture was then allowed to warm to room temperature overnight, resulting in a suspension of a yellow solid in a brown solution. A final portion of $NaC_{10}H_8$ (3 mL, 0.315 N in THF, 0.95 mmol) was added to the mixture at 0 °C, causing it turn green (the solid remained yellow). The suspension was refluxed for 2 h and then allowed to stand at room temperature overnight. The solid was separated from the solution (containing quite pure **8**) and extracted with fresh THF (100 mL) over 2 d, resulting in a yellow suspension which was allowed to stand overnight before collecting and drying in vacuo to yield yellow **5**·6C_4H_8O (2.91 g, 37.5%). Anal. Calcd for $C_{112}H_{152}Cl_2Na_2O_{14}W_2$: C, 60.95; H, 6.94. Found: C, 61.04; H, 7.20. ^{1}H NMR (Py-d_5, 323 K, ppm): δ 7.22 (s, Ar H), overlapping with Py-d_5, 7.03 (s, 8H, Ar H), 4.93 (d, J = 13.7 Hz, 8H, endo CH_2), 3.65 (m, 24H, THF), 3.46 (d, J = 13.7 Hz, 8H, exo CH_2), 1.64 (m, 24H, THF), 1.29 (s, 36H, Bu^t), 0.98 (s, 36H, Bu^t). The solid recrystallized from Py/THF gave crystals of [{*p*-Bu^t-calix[4]-$(O)_4$}$_2$$W_2${Na(thf)(Py)}$_2$($\mu$-Cl)$_2$]·1.6Py·0.2THF (a different solvated form) suitable for X-ray analysis.

Synthesis of 7. A solution of **6** (2.2 g, 2.6 mmol) in toluene (100 mL) was irradiated with a Xe lamp (540 W/m^2 at 340 nm) for 60 h. Bu^{t}NC (0.22 g, 2.6 mmol) was added to the resulting black suspension, yielding, after overnight stirring, a suspension of a violet solid in a reddish solution. The solid was collected and dried in vacuo to give **7**·2C_7H_8 (1.42 g, 54%). Anal. Calcd for $C_{112}H_{138}N_2O_8W_2$: C, 66.99; H, 6.92; N, 1.39. Found: C, 66.83; H, 6.82; N, 1.19. ^{1}H NMR ($CDCl_3$, 298 K, ppm): δ 7.3−7.08 (m, 26H, Ar H, tol), 4.90 (d, 4H, J = 12.7 Hz, endo CH_2), 4.63 (d, 4H, J = 12.2 Hz, endo CH_2), 3.42 (d, 4H, exo CH_2), overlapping with 3.33 (d, 4H, exo CH_2), 2.40 (s, 6H, tol), 1.31 (s, 18H, Bu^t), 1.25 (s, 36H, Bu^t), 1.23 (s, 18H, Bu^t), −0.03 (s, 18H, Bu^{t}NC). IR (Nujol, ν_{max}/cm^{-1}): 2202.8 (s). Crystals suitable for an X-ray diffraction study were obtained in C_6D_6.

Synthesis of 8. **2**·2C_7H_8 (19.18 g, 17.7 mmol) was stirred with Na (1.22 g, 53 mmol) in THF (300 mL) overnight. The resulting green suspension was filtered, THF was evaporated in vacuo, DME was added, and the resulting mixture was refluxed for 3 h. **8**·5$C_4H_{10}O_2$ was then collected and dried in vacuo as a shiny green-brown solid (13.0 g, 68%). Anal. Calcd for $C_{108}H_{154}Na_2O_{18}W_2$: C, 60.22; H, 7.20. Found: C, 60.20; H, 7.42. ^{1}H NMR (CD_3CN, 298 K, ppm): δ 7.11 (s, 16H, Ar H), 4.92 (d, J = 11.2 Hz, 8H, endo CH_2), 3.52 (s, 20H, DME), 3.34 (s, 30H, DME), 3.20 (d, J = 11.2 Hz, 8H, exo CH_2), 1.21 (s, 72H, Bu^t). The solid recrystallized from Py/THF gave crystals of [{*p*-Bu^t-calix[4]-(O_4)}$_2$$W_2${$\mu$-Na(Py)$_2$}{$\mu$-Na(Py)$_3$}], a different solvated form, suitable for X-ray analysis.

Synthesis of 9. **2**·2C_7H_8 (8.71 g, 8.03 mmol) was stirred with Na (0.55 g, 23.9 mmol) in THF (300 mL) overnight. The resulting green suspension was refluxed for 3 h, NaCl was filtered off, Na (0.2 g, 8.7 mmol) was added, and the mixture was stirred at room temperature for 3 d, turning blue. Excess Na was filtered off, THF was evaporated to 20 mL, and pentane (100 mL) was added. Deep blue **9**·10C_4H_8O was then collected and dried in vacuo (3.0 g, 30%). Anal. Calcd for $C_{128}H_{184}Na_4O_{18}W_2$: C, 62.23; H, 7.50. Found: C, 62.30; H, 7.72. ^{1}H NMR (THF-d_8, 298 K, ppm): δ 6.88 (s, 16H, Ar H), 5.22 (d, J = 10.5 Hz, 8H, endo CH_2), 2.95 (d, J = 10.5 Hz, 8H, exo CH_2), 1.15 (s, 72H, Bu^t). Crystals suitable for an X-ray diffraction study were grown from THF/toluene at −25 °C.

X-ray Crystallography for Complexes 2, 4, 5, 7, 8, and 9. Single crystals suitable for X-ray diffraction were grown from common organic solvents (Table 1). Data for **2** were collected on a Philips PW1100 diffractometer, those for **4**, **5**, **7**, and **8** on a Rigaku AFC6S diffractometer, and those for **9** on a MAR345 image plate using Mo Kα radiation. The solutions and refinements were carried out using the programs SHELX76[10] and SHELX93.[11] The details of the X-ray data collection, structure solution, and refinement are given in the Supporting Information.[12]

(6) Giannini, L.; Solari, E.; Zanotti-Gerosa, A.; Floriani, C.; Chiesi-Villa, A.; Rizzoli, C. *Angew. Chem., Int. Ed. Engl.* **1997**, *36*, 753.
(7) Arduini, A.; Casnati, A. In *Macrocycle Synthesis*; Parker, O., Ed.; Oxford University Press: New York, 1996; Chapter 7.
(8) Giannini, L.; Solari, E.; Floriani, C.; Chiesi-Villa, A.; Rizzoli, C. *J. Am. Chem. Soc.* **1998**, *120*, 823.
(9) (a) Cintas, P. *Activated Metals in Organic Synthesis*; CRC: Boca Raton, FL, 1993. (b) *Active Metals*; Fürstner, A., Ed.; VCH: Weinheim, Germany, 1996.

Table 1. Experimental Data for the X-ray Diffraction Studies on Crystalline Complexes **5**, **7**, **8**, and **9**

	5	**7**	**8**	**9**
formula	$C_{106}H_{130}Cl_2N_2Na_2O_{10}W_2 \cdot 1.6C_5H_5N \cdot 0.2C_4H_8O$	$C_{98}H_{122}N_2O_8W_2 \cdot 2C_6H_6$	$C_{113}H_{129}N_5Na_2O_8W_2 \cdot 2C_4H_8O$	$C_{120}H_{168}Na_4O_{16}W_2 \cdot 2C_4H_8O$
a, Å	14.177(3)	13.054(2)	24.962(3)	23.407(3)
b, Å	19.803(4)	19.044(4)	34.877(4)	26.830(2)
c, Å	20.896(4)	21.239(4)	12.869(2)	23.780(3)
α, deg	90	90	90	90
β, deg	97.97(2)	106.41(2)	90	90
γ, deg	90	90	90	90
V, Å^3	5810(2)	5064.9(17)	11204(3)	14934(3)
Z	2	2	4	4
fw	2217.8	1980.0	2243.2	2470.5
space group	$P2_1/c$	$P2_1/c$	*Pnma*	$Cmc2_1$
t, °C	−138	22	22	22
λ, Å	0.710 69	0.710 69	1.541 78	0.710 69
ρ_{calc}, g cm^{-3}	1.268	1.298	1.330	1.099
μ, cm^{-1}	21.26	23.70	43.02	16.33
transm coeff	0.775−1.000	0.722−1.000	0.843−1.000	0.632−1.000
R^a	0.072	0.064	0.044	0.054 [0.066]^b
$R_w{}^c$	0.182	0.186	0.131	0.141 [0.181]
GOF	1.035	0.983	0.993	1.049
N-observed^d	6285	4865	4376	13068
N-independent^e	8271	11 620	10 773	15 329
N-refinement^f	6285	9106	8381	13 068
no. of variables	579	514	639	696

^{a} $R = \sum|\Delta F|/\sum|F_o|$, calculated on the observed reflections. ^{b} Values in brackets refer to the "inverted" structure. ^{c} $R_w = [\sum w|\Delta F^2|^2/\sum w|F_o{}^2|^2]^{1.2}$. ^{d} *N*-observed is the total number of the independent reflections having $I > 2\sigma(I)$. ^{e} *N*-independent is the number of independent reflections. ^{f} *N*-refinement is the number of reflections used in the refinement having $I > 0$ for **7**, **8** and $I > 2\sigma(I)$ for **5**, **9** and corrected for absorption.

Results and Discussion

Complex **2** is the kinetic product of the reaction between [*p*-Bu^t-calix[4]-(OH)$_4$], **1**, and [WCl_6]. Suspensions of **2** are thermally very stable, but Lewis acidic metal chlorides (WCl_6, $AlCl_3$) catalyze its transformation into the trans isomer, [*trans*-Cl_2W{*p*-Bu^t-calix[4]-(O)$_4$}], **3**. The chemistry of **3**, still under investigation, is very different from that of **2**, and in order to obtain pure products in the derivatization of the latter, the presence of the former must be avoided. A reliable preparation protocol for both isomers has been developed, as outlined in Scheme 1. The higher thermodynamic stability of the trans isomer can be rationalized in terms of conformational strain of the calix moiety. In the cis complex, the calix[4]arene assumes an elliptical cross-section conformation with one couple of opposite phenyl rings pushed outward from and the other inward toward the cavity; in solution, a C_{2v}-symmetric NMR spectrum is observed. On the other hand, in the trans complex, the ligand assumes its favorite regular cone conformation, which leads to a C_{4v} NMR spectrum. The X-ray analysis for complex **2** is included in the Supporting Information.

Reductions of [*cis*-Cl_2W{*p*-Bu^t-calix[4]-(O)$_4$}]: Formation of W−W Bonds. Complex **2** undergoes controlled reduction according to Scheme 2, leading to a number of structurally interesting compounds.

When the reduction was carried out in a K:W 1:1 molar ratio, no salt separation was observed, and the paramagnetic tungsten(V) derivative **4** was obtained. The magnetic analysis suggested that the complex was a monomer, μ_{eff} being only slightly dependent on temperature (μ_{eff} = 1.3−1.9 for T = 1.9−300 K), as is usually found for complexes having large spin−orbit contributions.[13] In the ^{1}H NMR spectrum, spread over 25 ppm, two singlets around 1.2 ppm, tentatively assigned to the Bu^t groups (which are expected to be the least affected by paramagnetic shifts), suggested a C_{2v} symmetry for **4**, which was confirmed by the X-ray analysis, which is reported in the Supporting Information. The most interesting structural feature of **4**, overall quite similar to the parent compound **2**, is the unusual complexation inside the calix[4]arene cavity of K^+, whose solvation is partially provided by η^6-bonded opposite phenyl rings (see Supporting Information). A similar solvation

Scheme 2

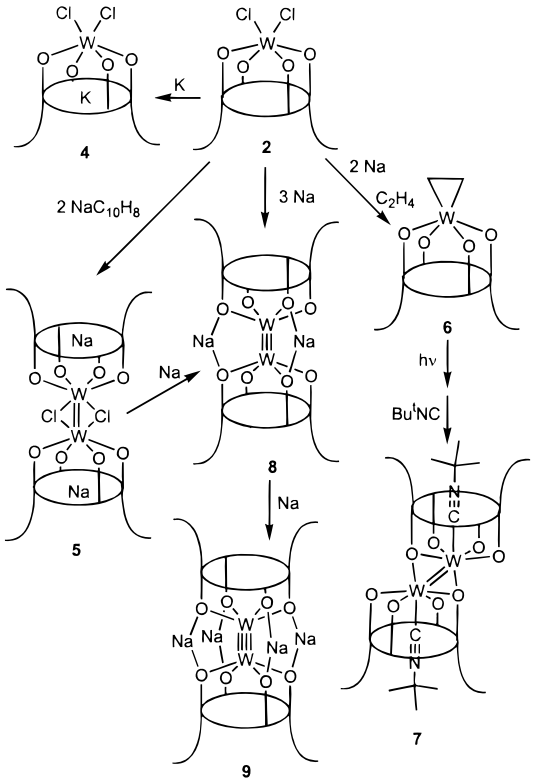

(10) Sheldrick, G. M. *SHELX76: Program for crystal structure determination*; University of Cambridge: Cambridge, U.K., 1976.
(11) Sheldrick, G. M. *SHELXL93: Program for crystal structure refinement*; University of Göttingen: Göttingen, Germany, 1993.
(12) See paragraph at end of paper regarding Supporting Information.
(13) Boudreaux, E. A.; Mulay, N. L. *Theory and Applications of Molecular Paramagnetism*; Wiley: New York, 1976; p 148.

Chart 1

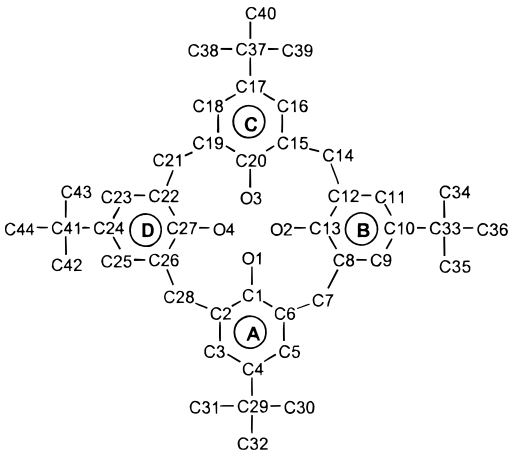

mode of K^+ was structurally identified in tantalum−alkali cation calix[4]arene complexes.[14] The solvation of alkali metal cations by π-interacting hydrocarbon moieties[15] recently attracted remarkable interest.

Increasing the reducing agent:W ratio and using sodium naphthalenide led to the isolation of the two-electron-reduced, diamagnetic compound **5**. Experimentally, more than 2 equiv of Na was actually employed, yielding a mixture of **5** and **8**, from which pure **5** could be obtained. On the other hand, using 2 equiv of sodium naphthalenide, **5** is formed together with a violet, uncharacterized product of similar solubility, which makes purification problematic (the resulting violet mixtures can be reduced cleanly to **8**).

The C_{2v} symmetry of the ^{1}H NMR spectrum and the elemental analysis, showing the presence of one formula unit of NaCl per W, suggested for **5** the structure sketched in Scheme 2, which was confirmed by an X-ray analysis. The labeling scheme adopted for the W{*p*-Bu^t-calix[4]-(O)$_4$} moiety for all complexes is indicated in Chart 1. Selected bond distances and angles are given in Table 2. In Table 3 a comparison of relevant conformation parameters within the W{*p*-Bu^t-calix[4]-(O)$_4$} units is reported.

The structure of **5** consists of [W$_2${*p*-Bu^t-calix[4]-(O)$_4$}$_2${Na(Py)(thf)}$_2$(μ-Cl)$_2$] centrosymmetric dimers (Figure 1) showing a W═W [2.614(1) Å] double bond. The W−Cl−W′ angle is rather narrow [65.0(1)°], in agreement with the formation of the metal−metal double bond. The direction of the W═W′ bond is perpendicular to the reference plane [dihedral angle between the W−W line and the normal to the plane being 0.9(1)°], so that the two centrosymmetric W{*p*-Bu^t-calix[4]-(O)$_4$} fragments overlap. The six-coordination of the metal and the inclusion of the alkali metal cation removes the planarity of the O$_4$ core and the cone conformation of the calix[4]arene, the opposite A and C rings being nearly parallel to each other and to the reference plane in a conformation very close to that observed in **4** (Supporting Information). The sodium cation, which is solvated by O(1), O(3), O(5)$_{THF}$, and N(1)$_{Py}$, is in addition η^3-bonded to the D ring [Na···C(22) 2.226(14), Na···C(26) 3.212(14), Na···C(27) 3.096(15) Å]. The different mode of coordination of the alkali ion in the cavity with respect to complex **4** seems due mostly to the alkali metal cation, as roughly the same behavior (η^3-coordination of Na^+ vs η^6-coordination of K^+) has been observed in [{*p*-Bu^t-calix[4]-(O)$_4$-Ta(OAr)$_2$}{ML$_n$}] [M = alkali metal cation] complexes.[14] In the same paper,[14] it was also shown that additional solvent molecules coordinated to the alkali metal ion in the cavity can be easily removed without major changes in the structure of the complexes. This makes us confident that the different solvated forms (THF and THF/Py) of complex **5** would not exhibit significant structural differences.

As discussed elsewhere, when the reduction of the parent compound **2** was conducted at low temperature (−20 °C) with 2 equiv of Na in THF saturated with ethylene, complete salt removal was achieved, and the η^2-ethylene complex **6** could be isolated.[8] Upon irradiation, the latter released ethylene, behaving as a source of the d^2 [W{*p*-Bu^t-calix[4]-(O$_4$)}] carbenoid, which coupled to give a new W═W dimer, isolated as the bis-Bu^{t}NC adduct **7**. In ^{1}H NMR, **7** exhibits a C_s-symmetric pattern of signals for the calix[4]arene moiety; guest

Table 2. Selected Bond Distances (Å) and Angles (deg) for Complexes **5**, **7**, **8**, and **9**

	Complex **5**[a]		
W(1)−O(1)	2.002(7)	W(1)−Cl(1)	2.431(3)
W(1)−O(2)	1.976(8)	W(1)−Cl(1)′	2.434(3)
W(1)−O(3)	2.009(8)	W(1)−W(1)′	2.614(1)
W(1)−O(4)	1.986(8)	Cl(1)−W(1)−Cl(1)′	115.0(1)
	Complex **7**[a]		
W(1)−W(1)′	2.582(1)	W(1)−C(45)	2.188(11)
W(1)−O(1)	1.950(8)	N(1)−C(45)	1.130(13)
W(1)−O(2)	2.004(7)	O(2)′−W(1)−C(45)	176.1(4)
W(1)−O(2)′	2.052(6)	W(1)−C(45)−N(1)	178.6(10)
W(1)−O(3)	1.978(8)	W(1)−O(2)−W(1)′	79.1(2)
W(1)−O(4)	1.953(8)	O(2)′−W(1)−O(2)	100.9(3)
	Complex **8**[b]		
W(1)−W(1)′	2.313(1)	W(1)−O(4)	2.017(5)
W(1)−O(1)	2.015(5)	Na(1)−O(4)	2.277(7)
W(1)−O(2)	1.960(5)	Na(2)−O(1)	2.357(7)
W(1)−O(3)	1.936(5)		
	Complex **9**[c]		
W(1)A−W(1)B	2.292(1)	Na(1)−O(2)A	2.182(6)
W(1)−O(1)	2.097(5)	Na(2)−O(2)B	2.167(6)
W(1)−O(2)	2.102(5)	Na(2)−O(1)A	2.173(7)
Na(1)−O(1)B	2.178(7)		

[a] A prime denotes a transformation of $-x, -y, -z$. [b] A prime denotes a transformation of x, 0.5 − y, z. [c] A prime denotes a transformation of $-x, y, z$.

Table 3. Comparison of Relevant Conformational Parameters within Calix[4]arene for Complexes **5**, **7**, **8**, and **9**

	5	**7**	**8**	**9**
(a) Distances (Å) of Atoms from the O$_4$ Mean Plane				
O(1)		−0.040(8)	−0.014(7)	0(−)
O(2)		0.029(7)	0.015(7)	0(−)
O(3)		−0.041(8)	−0.015(7)	0(−)
O(4)		−0.037(8)	0.015(7)	0(−)
W		−0.115(1)	0.317(1)	0.457(1)
(b) Dihedral Angles (deg) between Planar Moieties[a]				
E−A	172.9(3)	125.2(3)	121.4(2)	120.9(2)
E−B	116.1(3)	128.4(3)	121.4(2)	122.0(2)
E−C	170.3(3)	128.8(3)	129.2(2)	122.0(2)
E−D	117.4(3)	123.3(3)	123.5(2)	120.9(2)
A−C	163.3(4)	106.0(4)	109.5(3)	117.1(3)
B−D	126.5(4)	108.2(4)	115.1(2)	117.1(3)
(c) Contact Distances (Å) between Para-Carbon Atoms of Opposite Aromatic Rings[b]				
C(4)···C(17)	10.75(2)	8.668(19)	8.503(15)	8.230(13)
C(10)···C(24)	7.535(19)	8.694(20)	8.227(14)	8.230(13)

[a] E (reference plane) refers to the least-squares mean plane defined by the C(7), C(14), C(21), C(28) bridging methylenic carbons. [b] For complex **9**, C(17) and C(24) should be read C(10)′ and C(4)′, respectively; a prime denotes a transformation of $-x, y, z$.

(14) Zanotti-Gerosa, A.; Solari, E.; Giannini. L.; Floriani, C.; Chiesi-Villa, A.; Rizzoli, C. *Chem. Commun.* **1997**, 183 and references therein.
(15) Ma, J. C.; Dougherty, D. A. *Chem. Rev.* **1997**, *97*, 1303.

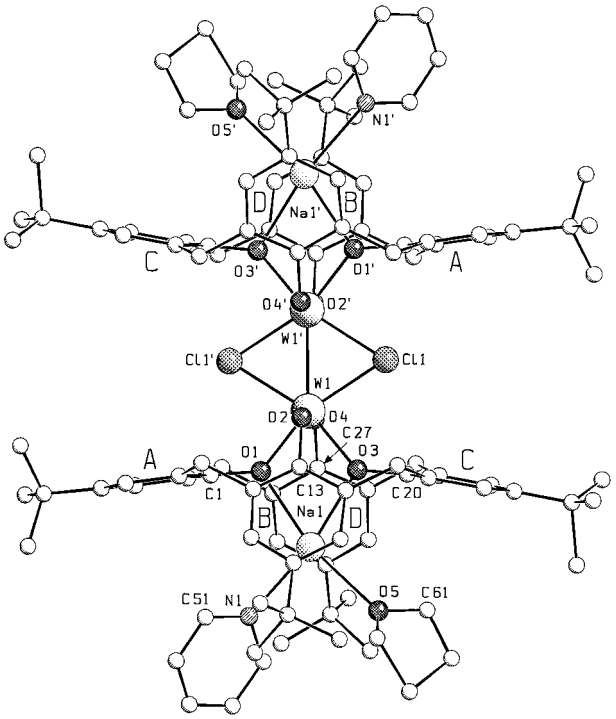

Figure 1. SCHAKAL view of complex **5**. Disorder affecting the butyl groups associated with the A and C rings and with the THF molecule has been omitted for clarity. A prime denotes a transformation of $-x$, $-y$, $-z$.

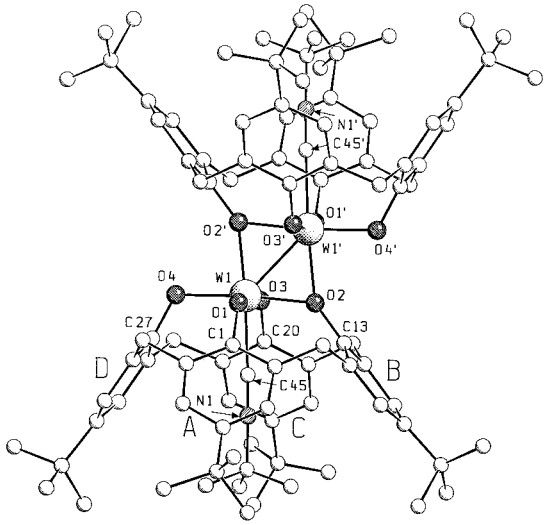

Figure 2. SCHAKAL view of complex **7**. Disorder affecting the butyl groups associated with the **B** and **C** rings has been omitted for clarity. A prime denotes a transformation of $-x$, $-y$, $-z$.

protons give the expected high-field resonance (-0.03 ppm).[16] The coordination is irreversible and leads to a shift of C$-$N stretching to high frequences (2203 cm^{-1}), indicating that tungsten behaves as a net electron acceptor (no back-donation is to be expected as the two electrons of tungsten are engaged in the M$=$M double bond).

The centrosymmetric dimer **7** is shown in Figure 2 [W$=$W 2.582(1) Å]. Coordination around the metal involves the O_4 core and two additional trans ligands provided by the O(2′) oxygen atom and by the C(45) atom from a Bu^{t}NC molecule. The W$-$O(2)$-$W′ angle is rather narrow [79.1(2)°], in agreement with the formation of the metal$-$metal double bond. The O_4 core is planar, the metal atom being displaced by 0.115(1) Å toward the O(2′) oxygen, and forms a dihedral angle of 48.8(1)° with the direction of the W$=$W bond. As expected for complexes with six-coordinated metal atoms having two additional trans ligands, calix[4]arene exhibits a cone section conformation (Table 3). The W$=$W and W$-$O bond lengths fall in the usual range (Table 2).

As described elsewhere, **7** is also obtained by reacting [{*p*-Bu^t-calix[4]-(O)$_4$}W$=$C(H)R] species with Bu^{t}NC.[17] The different genesis of **5** and **7**, both containing a W$-$W double bond in an edge-sharing bioctahedron, clearly indicates that the W$=$W functionality requires the support of two bridging ligands, either chlorides (see **5**) or oxygens of adjacent metalla-calix[4]arene moieties (see **7**).

The reduction of **2** with 3 equiv of Na gave complex **8**. Elemental analysis indicated complete salt removal, and in solution, a C_{4V} ^{1}H NMR spectrum was observed, which led to the conclusion that **8** was a dimer, with a triple metal$-$metal bond.

Complex **8** was isolated as a DME solvate and crystallized as a Py solvate, with THF in the cavity. As the different solvations affect only the Na cations, we suppose that the two forms share the same fundamental structure. When excess Na is added to a THF solution of **8**, an addition 1 equiv of Na per W atom is consumed. The resulting deep blue W^{II} compound, **9**, was found to be diamagnetic in the solid state by a SQUID analysis. Despite the high reactivity of **9** toward a number of substrates, including some solvents, a genuine ^{1}H NMR spectrum of **9** could be obtained in THF-d_8, showing a C_{4V} pattern for the calix[4]arene moiety and the diamagnetism of the complex.

Among the properties of the electron-rich metalla-calix[4]arene dimers mentioned above, we should emphasize their occurrence in the ion-pair form, with alkali metal cations tightly bonded to the calix[4]arene fragments. The alkali metal cations in such structures have very different binding sites, either displaying a bridging bonding mode across the lower rims of two adjacent calix[4]arenes, as in **8** and **9**, or being complexed inside the cavity, as in **4** and **5**, where they experience η^6 or η^3 interactions with the arene rings. The electronic structure of the dimers **5**$-$**9** will be discussed in the part dedicated to extended Hückel calculations (vide infra).

The structures of **8**, recrystallized from pyridine, and **9** are discussed jointly, due to their similarity, and they are displayed in Figures 3 and 4, respectively.

Both dimers contain a tungsten$-$tungsten multiple bond (2.313(1) and 2.292(1) Å in **8** and **9**, respectively), is consistent with a triple bond in **8** and eventually a quadruple bond in **9**. Both complexes possess crystallographically imposed C_s symmetry, the mirror plane running through the sodium cations and the midpoint of the W$-$W bond in **8** and through the tungsten atoms and the C(14), C(28) bridging methylene carbon atoms in **9**. Values hereinafter reported refer to molecule A of complex **9**. Values of molecule B are given in the Supporting Information. The metals are displaced from the planar O_4 cores by 0.317(1) and 0.457(1) Å for **8** and **9**, respectively (Table 3). The W$-$W′ line forms dihedral angles of 4.5(2) and 0.1(1)° with the normal to the O_4 planes. Considering the environment of the two metal atoms as a whole, the coordination environment of the W≡W unit is a tetragonal prism, in which the tungsten atoms lie at the center of two faces, and the dihedral angles between the

(16) Acho, J. A.; Doerrer, L. H.; Lippard, S. J. *Inorg. Chem.* **1995**, *34*, 2542.

(17) Giannini, L.; Solari, E.; Dovesi, S.; Floriani, C.; Re, N.; Chiesi-Villa, A.; Rizzoli, C. *J. Am. Chem. Soc.*, in press.

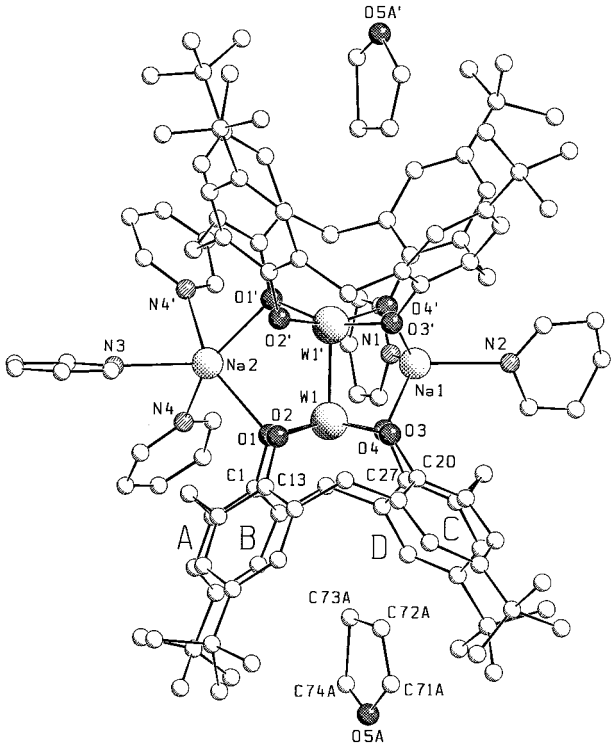

Figure 3. SCHAKAL view of complex **8**. Disorder affecting the butyl groups associated with the **C** ring, the THF molecule, and the pyridine molecules has been omitted for clarity. A prime denotes a transformation of x, $0.5 - y$, z.

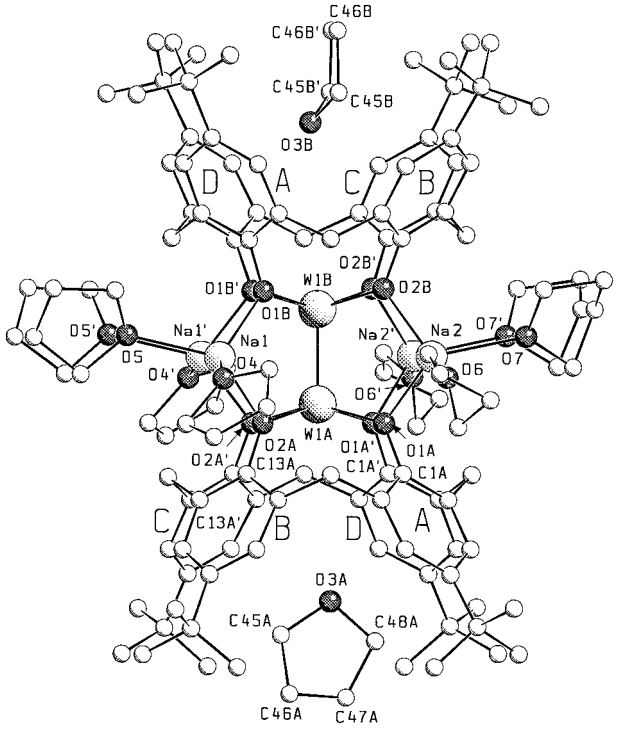

Figure 4. SCHAKAL view of complex **9**. Disorder affecting the THF molecules has been omitted for clarity. A prime denotes a transformation of $-x$, y, z.

two O_4 cores are 9.0(2) and 1.1(1)° for **8** and **9**, respectively. The W−O bond distances fall in the usual range (Table 2). In complex **8**, the Na(1) and Na(2) cations, which lie on the mirror plane, are anchored to the dimer by bridging the symmetry-related O(4), O(4′) and O(1), O(1′) pairs of atoms, respectively. Coordination is completed to distorted tetrahedral by the nitrogen

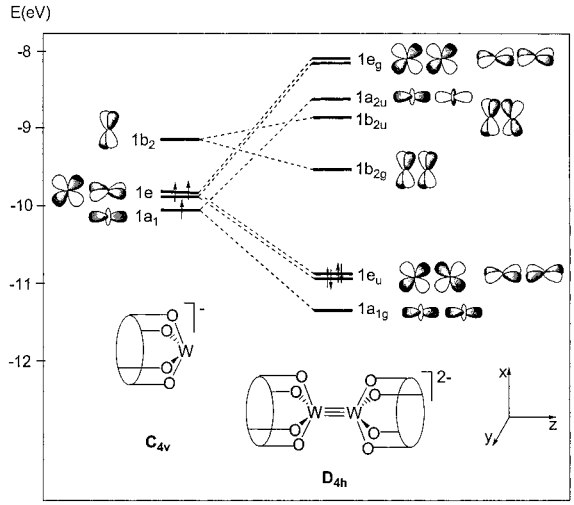

Figure 5. Molecular orbital interaction diagram for **8**.

atoms of two pyridine molecules for Na(1) and to distorted trigonal bipyramidal by the nitrogen atoms of three pyridine molecules for Na(2). In complex **9**, the Na(1) and Na(2) cations bridge the O(2)A, O(1)B and O(1)A, O(2)B pairs of atoms, respectively.

In the structure of an analogous compound recently reported by Chisholm, H^+ and $Me_2NH_2^+$ act as bridging cations, while the W−W distance is 2.3039(8) Å.[5] It is worth noting that a similar arrangement of eight monodentate alkoxide ligands around a W_2^{6+} core to form a pseudo-O_8 cube had been reported by the same author, with a W−W distance of 2.335(1) Å.[18]

Extended Hückel Analysis. Extended Hückel calculations[19] were performed to elucidate the electronic structure of some of the considered compounds, notably the metal−metal-bonded species **5**, **7**, **8**, and **9**.

Some the considered compounds are quite complicated di- or tetraanionic species involving two or four Na^+ countercations coordinated to the ligand oxygen atoms and further coordinated by solvent molecules. In our calculations, these structures were simplified by the removal of the Na^+ ions and the solvent molecules, thus extracting the basic dianionic and tetraanionic units. Although the Na^+ ions do contribute to the thermodynamic stability of the actual molecules, their effect is essentially electrostatic and is not expected to affect significantly the electronic structure of the W_2 core. Moreover, the calix[4]arene ligands have been slightly simplified by replacing the Bu^t groups and the methylene bridges by hydrogens and symmetrizing to a C_{4v} or C_{2v} local symmetry. This simplified model retains the main features of the whole ligand; in particular, the geometrical constraints on the O_4 set of donors atoms have been maintained by fixing the geometry of the four phenoxo groups to the experimental X-ray values.

We first considered the metal−metal-bonded complexes **8** and **9**, analyzing their electronic structures in terms of the interactions between the frontier orbitals of two $[W(calix)]^-$ or $[W(calix)]^{2-}$ fragments, respectively. The frontier orbitals of the $[W(calix)]^-$ fragment are shown on the left in Figure 5 and consist of four low-lying metal-based orbitals. The $d_{x^2-y^2}$ orbital, pointing more closely toward the oxygen ligands, is pushed high in energy while the remaining four d orbitals are found within 0.8 eV. The lowest energy metal orbital is a $1a_1$ (d_{z^2}) orbital

(18) Chisholm, M. H.; Folting, K.; Huffman, J. C.; Streib, W. E. *J. Am. Chem. Soc.* **1995**, *117*, 7428.
(19) Hoffmann, R.; Lipscomb, W. N. *J. Chem. Phys.* **1962**, *36*, 2179. Hoffmann, R. *J. Chem. Phys.* **1963**, *39*, 1397.

with a doubly degenerate 1e (d_{xz}, d_{yz}) orbital ca. 0.2 eV above. Due to the π interactions with the oxygen atoms, the $1b_2$ (d_{xy}) orbital lies ca. 0.6 eV higher in energy. For such a W(III) fragment with a d^3 electron count, these orbitals are occupied by three electrons as shown in Figure 5. The interaction between the two $[W(calix)]^-$ fragments in **8** is illustrated by the molecular orbital diagram on the right in Figure 5, showing a W−W $\sigma^2\pi^4$ configuration and indicating a metal−metal triple-bond character, consistent with the observed metal−metal distance of 2.313 Å. For the tetraanionic dimer **9**, which differs from **8** by two more electrons, on the basis of the molecular orbital scheme in Figure 5, we would expect a formal $\sigma^2\pi^4\delta^2$ configuration with a metal−metal quadruple bond and a shorter W−W bond length. However, the strong π donation from the oxygen p_π to the tungsten d_{xy} orbitals leads to a significant destabilization of the latter orbitals, involved in the W−W δ bonding. The contribution to the metal−metal bond from the occupied δ orbital is therefore very weak, in agreement with the observed W−W bond distance in **9**, 2.27 Å, which is only negligibly shorter than that in **8**, despite the higher formal metal−metal bond order. The high energy of the occupied δ orbital also explains the high reactivity of **9**, in particular toward oxidation. It is worth noting that no quadruply bonded $(W-W)^{4+}$ compound supported by alkoxide or phenoxide ligands is known,[20] so that **9** is unprecedented. However, a few $(Mo-Mo)^{4+}$ compounds, $Mo_2(OR)_4L_4$ (L = R′OH, Py, PMe_3), are known and show metal−metal distances (2.10−2.20 Å) slightly shorter than or almost identical to those observed (2.20−2.25 Å) for the triply bonded $(Mo-Mo)^{6+}$ compounds, such as $Mo_2(OR)_6$.[20,21]

We then turned our attention to compounds **5** and **7**. For these $(W-W)^{8+}$, d^2-d^2 compounds with an edge-sharing distorted octahedral structure, a double bond is expected on the basis of the simple qualitative model usually assumed for this class of complexes[1,22] and is supported by the W−W bond lengths of 2.614 and 2.583 Å, respectively, which fall in the range of W−W double bonds.[1] The interaction diagram in Figure 6 illustrates the building up of the molecular orbitals of the dianion $[W_2(\mu\text{-Cl})_2\{p\text{-Bu}^t\text{-calix[4]-(O)}_4\}_2]^{2-}$ in **5**, starting from the $[W(calix)]_2$ and $(Cl)_2^{2-}$ fragments. The frontier orbitals of the former are reported on the left in Figure 6 and consist essentially of the same M−M bonding and antibonding orbitals of **8** and **9** illustrated on the right in Figure 5. However, due to the lower symmetry of the [W(calix)] units in **5**, the doubly degeneracy of the π and π^* orbitals observed in **8** and **9** is not maintained. The frontier orbitals of $(Cl)_2^{2-}$ are reported on the right in Figure 6 and correspond essentially to the suitable combinations of Cl^- atomic orbitals. Figure 6 shows a significant match between some of the orbitals of $[W(calix)]_2$ with metal−metal character and the orbitals of the $(Cl)_2$ unit. In particular, this competition between W ligands and W−W interactions leads to a reversal of the $\delta-\delta^*$ ordering and to a significant chlorine contribution to the σ and π_y orbitals. The overall electron configuration is essentially $\sigma^2\pi^2$, thus supporting a tungsten−tungsten double bond in **5**. However, the partial chlorine character of the σ and π_y orbitals weakens their contribution to the metal−metal bond (as shown by the decrease in the W−W overlap population from 0.61 in $[W(calix)]_2$ to 0.47 in **5**), in agreement with the observed W−W bond length, which is higher than that observed in other

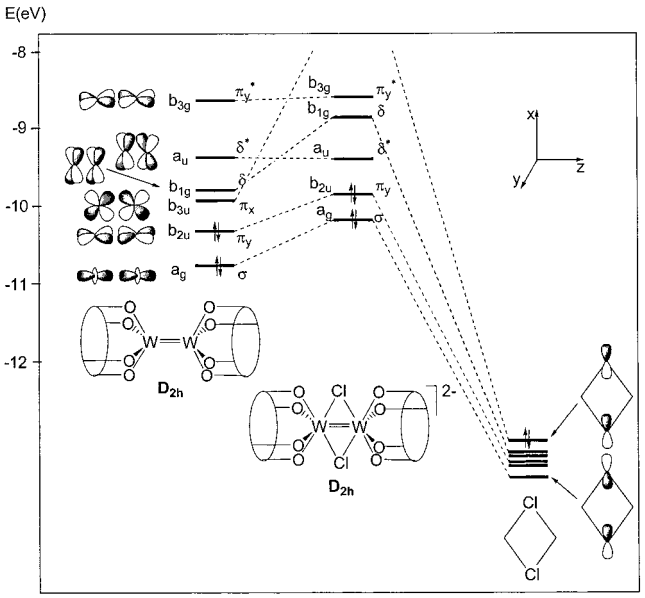

Figure 6. Molecular orbital interaction diagram for **5**.

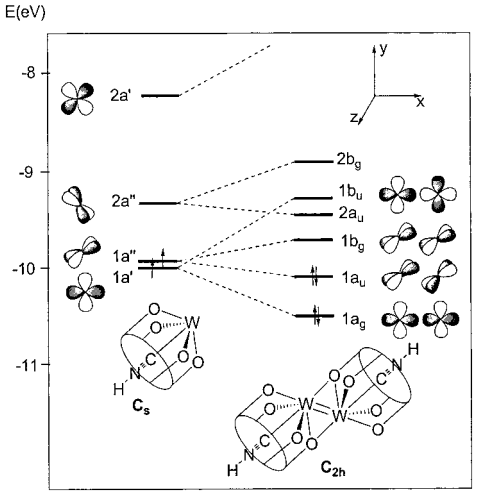

Figure 7. Molecular orbital interaction diagram for **7**.

$(W-W)^{8+}$ compounds with less interacting bridging ligands, such as OR^-.[1,23]

An analogous $\sigma^2\pi^2$ configuration still supporting a tungsten−tungsten double bond is found for **7**, although the analysis of the electronic structure is complicated by the lower C_{2h} symmetry. Figure 7 illustrates the interaction diagram of **7** built in terms of two [{W(calix)(CNH)] units. The frontier orbitals of the square-pyramidal [W(calix)(CNH)] fragment (C_s) are reported on the left in Figure 7 and consist of three low-lying metal orbitals. The lowest metal orbital is 1a′ ($d_{x^2-y^2}$), which points mainly toward the missing oxygen ligand of the second fragment in the dinuclear species, while the two next orbitals, 1a″ and 2a″, are suitable combinations of the d_{xz} and d_{yz} orbitals with mainly π and δ character with respect to the W−isonitrile direction, respectively. The d_{xy} orbital is further destabilized by the π interaction with the oxygen ligands. The interaction of these orbitals gives rise to the corresponding bonding and antibonding combinations shown on the right in Figure 7 and therefore, for a d^2 electron count of the metal centers, to an essentially $\sigma^2\pi^2$ configuration. However, the $1a_u$ HOMO of

(20) Chisholm, M. H. In *Early Transition Metal Clusters with π-Donor Ligands*; Chisholm, M. H., Ed.; VCH: New York, 1995.
(21) Chisholm, M. H.; Folting, K.; Huffman, J. C.; Tatz, R. J. *J. Am. Chem. Soc.* **1984**, *106*, 1153. Chisholm, M. H.; Folting, K.; Huffman, J. C.; Putilina, E. F.; Streib, W. E.; Tatz, R. J. *Inorg. Chem.* **1993**, *32*, 3771.
(22) Cotton F. A. *Polyhedron* **1987**, *6*, 667.
(23) Anderson, L. B.; Cotton, F. A.; De Marco, D.; Fang, A.; Ilsley, W. H.; Kolthammer, B. W. S.; Walton, R. A. *J. Am. Chem. Soc.* **1981**, *103*, 5078.

mainly metal−metal π-bonding character has a significant δ character, which slightly weakens the metal−metal bond strength with respect to a pure $\sigma^2\pi^2$ configuration. This in agreement with the observed W−W bond length, which is slightly higher than that observed in other $(W-W)^{8+}$ compounds with alkoxo or phenoxo bridging ligands.[1,23]

Conclusion

The stepwise reductive coupling of [*cis*-Cl_2W{calix[4]-$(O)_4$}], **2**, which has been very rarely applied as synthetic methodology in the field, led to the formation of metal−metal-bonded metallacalix[4]arene dimers containing double, triple, and quadruple W−W bonds. An unusual aspect of the compounds reported is their occurrence in the ion-pair form, derived from the use of a tetraanionic macrocyclic ligand. The alkali metal cations are either hosted by the cavity or display bridging bonding modes across two calix[4]arene moieties, giving rise to bifunctional heterometallic structures. In the former case, the rather rare solvation of the alkali metal cation by the arene rings has been proved by X-ray analyses. An alternative synthetic methodology, taking advantage of the labilization of an alkylidene in the presence of an isocyanide or of an olefin by photolysis, gave rise to a neutral W═W dimer.

Acknowledgment. We thank the Fonds National Suisse de la Recherche Scientifique (Bern, Switzerland) (Grant No. 20-53336.98), Ciba Specialty Chemicals (Basel, Switzerland), and the Fondation Herbette (University of Lausanne) for financial support.

Supporting Information Available: ORTEP drawings, text and a table presenting details of the X-ray data collection and structure solution and refinement, and tables giving crystal data, atomic coordinates, isotropic and anisotropic displacement parameters, and bond lengths and angles for **2**, **4**, **5**, **7**, **8**, and **9** and SCHAKAL drawings for **2** and **4**. This material is available free of charge via the Internet at http://pubs.acs.org.

IC9811796